

Pt-Au Core/Shell Nanorods: Preparation and Applications as Electrocatalysts for Fuel Cells

Chen-Wei Liu*, Yu-Chen Wei* and Kuan-Wen Wang*

*National Central University, No.300, Zhongda Rd., Taoyuan, Taiwan, kuanwen.wang@gmail.com

ABSTRACT

In this study, carbon-supported Pt-Au nanorods with core/shell structures and excellent electrochemical performance are prepared successfully by a facile wet chemical reduction method. The morphology and electro-catalytic activity correlation, including surface states/structures dependent ORR and FAO performance of Pt-Au nanorods are also explored. The ORR activity and long-term durability of Pt-Au nanorods are both better than those of commercial Pt/C due to the Au alloying and the 1-D morphology. Besides, it can be observed that for Pt shell nanorods, the surface is completely composed of Pt species, exhibiting high CO oxidation activity. On the other hand, the PtAu shell nanorods consisting of Pt and Au surface species, specifically promote FAO. The Pt-Au nanorods with 1-D morphology may enhance the electrochemical activity of ORR, FAO and CO oxidation.

Keywords: Pt-Au nanorod, core/shell, oxygen reduction reaction, formic acid oxidation, CO oxidation

1 INTRODUCTION

Nanostructured materials have been applied as electrocatalysts for oxygen reduction reaction (ORR), formic acid oxidation (FAO), and alcohol oxidation in the energy field [1,2]. Recently, carbon supported Pt nanowires have exhibited superior performance for ORR due to their novel one-dimensional (1-D) morphologies [3]. Owing to their smooth crystal planes, which can balance the interface between exposed Pt atoms and the oxygen adsorbates, the 1-D Pt nanomaterials with higher aspect ratios, fewer lattice boundaries, and less amounts of defect sites on the surface than zero-dimensional (0-D) nanomaterials may display high ORR kinetics [2,4]. In addition, 1-D electrocatalysts have shown improved durability for long-term applications compared to 0-D nanoparticles, which suffer the irreversible oxidation of surface atoms on their defect sites [5]. Besides, 1-D nanomaterials with structural anisotropy can enhance catalysts utilization and mass transport characteristics by path directing effects, providing facile pathways for the electron transfer through reducing the number of nanoparticle interfaces [1,6].

Although the carbon supported Pt nanoparticles are the state-of-the-art electrocatalysts applied for the ORR at the cathode [7], Pt electrocatalysts are easy to dissolve and subsequently the Pt ions migrate to the solution in the acid electrolyte during operation condition. Therefore, the

addition of Au into the Pt catalysts is regarded as a promising way to suppress Pt dissolution during ORR and improve the long-term durability owing to the decrease in the oxophilicity and the change in Pt electronic properties [8,9]. In this study, we have successfully synthesized carbon-supported Pt-Au nanorods with core/shell structures by a facile wet chemical reduction method [10]. The morphology and electro-catalytic activity correlation, including surface states/structures dependent ORR and FAO performance of Pt-Au 1D nanomaterials are also explored.

2 EXPERIMENTAL SECTION

2.1 Preparation of Catalysts

The Pt-Au/C nanorods with the Pt/Au ratio of 3:1 and 45 wt % of metal loading were prepared via the formic acid reduction method. Two step of reduction routes were used to synthesized Pt-Au/C nanorods with core/shell structures. Aqueous solutions of H_2PtCl_6 (Alfa Aesar) and HAuCl_4 (Aldrich) with stoichiometric ratio of 3:1 were blended and deposited with different sequence at 340 K onto the commercial carbon black (Vulcan XC-72R). For instance, the solution of H_2PtCl_6 and carbon were first mixed and reduced by formic acid for 72 hours, and then Au precursor was reduced by formic acid for another 48 hours. The as-deposited catalysts were subsequently dried at 330 K for 24 h, and stored as fresh PtAu shell nanorods. On the contrary, the Pt shell nanorods were prepared by the initial reduction of Au precursor and following deposition of Pt. For comparison, the commercial Pt/C (TKK) catalysts with 50 wt % Pt loading were used.

2.2 Characterization of Catalysts

The exact compositions and metal loadings of the Pt-Au nanorods were examined by inductively coupled plasma-atomic emission spectroscopy (ICP-AES, Jarrell-Ash ICAP 9000) and thermal gravimetric analysis (TGA, Perkin Elmer TGA-7), respectively. The phases and structures of the nanorods were characterized by a Shimadzu X-ray diffractometer with a $\text{CuK}\alpha$ ($\lambda = 0.15406$ nm) radiation source generated at 40 kV and 25 mA and performed in a 2θ range of 20 and 80°. The morphologies of the Pt-Au nanorods were examined by a Jeol-2100 high resolution transmission electron microscope (HRTEM) with a LaB_6 electron gun and a field emission scanning electron microscope (SEM, FEI Nova Nano 230).

Electrochemical measurements were performed by a glassy carbon rotating disk electrode (RDE), a MSR rotator (Pine Instrument) and a microcomputer-controlled electrochemical analyzer (CHI700a, CH Instrument). The inks prepared by mixing of alloy catalysts and Nafion solution (5 wt %, DuPont) in 2-propanol were dispersed and deposited onto the glassy carbon RDE (0.196 cm² area). A Pt plate and a saturated calomel electrode (SCE) were used as the counter and reference electrodes, respectively. The electrolyte used was O₂ (99.999 %) saturated 0.5 M H₂SO₄ (Panreac) aqueous solution. Linear sweep voltammetry (LSV) was conducted at a scan rate of 5 mVs⁻¹ and a rotation rate of 1600 rpm. All potentials in this study are given with respect to the reference electrode, which is +0.241 V vs. NHE. The stability of the Pt-Au nanorods conducted via cyclic voltammograms (CV) characterization was recorded at a scan rate of 20 mVs⁻¹ in the N₂-saturated 0.5 M H₂SO₄ aqueous solution between 0 and 1.6 V.

3 RESULTS AND DISCUSSION

The exact metal loading and Pt/Au compositions of nanorods examined by the TGA and ICP-AES are 45.5 wt % and 74.2/26.8, respectively. The morphologies of Pt-Au core/shell nanorods characterized by SEM and HRTEM are shown in Figures 1. For the Pt shell nanorods, the bare carbon spheres (Vulcan XC-72R) with a diameter of 30 – 60 nm are covered randomly by nanorods. The TEM images display that the inherently anisotropic Pt shell nanorods with a length of 10 – 20 nm, are grown on the carbon spheres. The calculated interplanar lattice parameter of Pt shell is ~ 0.23 nm, consistent with the (111) lattice plane of bimetallic Pt-Au [11]. On the other hand, for the PtAu shell nanorods, the SEM and TEM images reveal that the PtAu shell nanorods have crystalline structure with an average length of 10-25 nm and the lattice parameter of 0.23 nm, also in agreement with the (111) lattice planes of bimetallic Pt-Au [11]. However, the core/shell components of Pt shell and PtAu shell are not easily distinguished by TEM because Au and Pt exhibit similar imaging contrast and have the same crystal structure [12].

Figure 2 shows the XRD patterns of Pt-Au nanorods. Based on the peak positions of face-centered cubic Pt (JCPDS #04-0802) and Au (JCPDS #04-0784) shown in the upper panels, the split peaks of Pt-Au nanorods can be indexed to the (111), (200), and (220) reflections of the Pt-rich and Au-rich alloys. For Pt shell and PtAu shell nanorods, the patterns have intensive Au-rich and Pt-rich peaks, respectively, suggesting that the initial nucleation component, forming the large crystalline core, contributes a lot to the pattern [13]. Moreover, by fitting the (111) split peaks of nanorods, the area ratios of Au-based peak to Pt-based peak is about 1 to 3, implying that the starting materials form these two distinct solid solutions with different sizes and compositions depending on the preparation route. In other words, for Pt shell nanorods, once the Au precursors are initially reduced on the carbon

nanospheres, the preferred orientation of (111) plane for metallic Au is strongly dominant and the large Au crystallites are rich in the inner core. On the contrary, for the PtAu shell, Pt crystallites enrich in the inner core while the outer shell is covered by Pt and some Au.

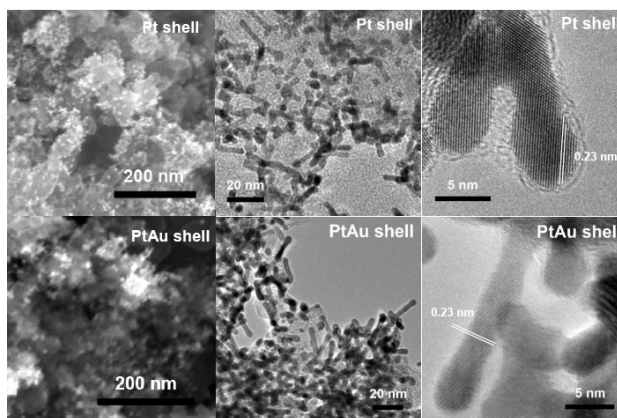


Figure 1: SEM and HRTEM images of Pt-Au nanorods.

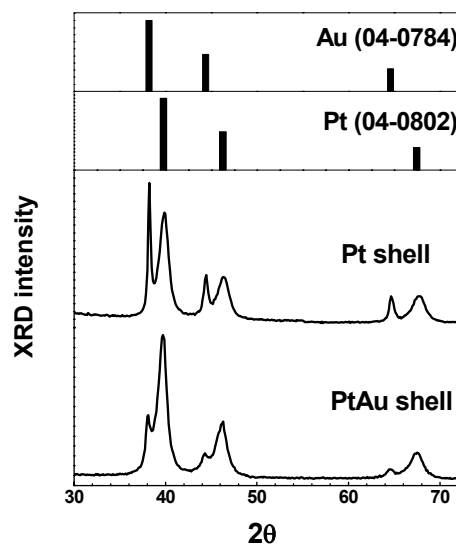


Figure 2: XRD patterns of the Pt-Au nanorods.

The core/shell structures of Pt-Au can be analyzed precisely by the CV curves, which can provide the information for assessing the relative surface enrichment of Pt and Au [14]. As displayed in Figure 3, the oxidation state of the surface atoms in each CV related to the applied potential can easily be determined, providing semiquantitative information on the composition of the outermost atomic layer of the electrode material [15]. For the typical voltammetric response of Pt and Au surface, the oxide stripping peak is located at 0.7 and 1.18 V, respectively [16,17]. As shown in Figure 3, the

characteristic peak of Au located at 1.18 V for PtAu shell nanorods is more significant than that for Pt shell, indicating that the surface Au of the former is richer than that of the latter, which reflects the molecular level information for oxide products directly obtained at the electrode-electrolyte interface. It can be observed that for Pt shell nanorods, the main reduction peak located at 0.68 V implies their surface is completely composed of Pt species, while the surface of PtAu shell nanorods consists of Pt and Au species, confirming the preparation route significantly affects the core/shell structure of the Pt-Au nanorods.

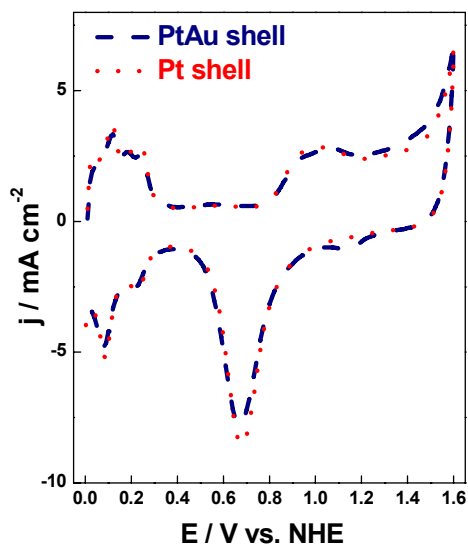


Figure 3: CV measurements of Pt-Au nanorods in 0.5 M H_2SO_4 .

The ORR kinetics of the Pt shell and PtAu shell nanorods before and after 50 cycles (denoted as L) are performed by rotating disk electrodes (RDE) and compared in Figure 4. Notably, the ORR activities of Pt-Au nanorods are both better than that of commercial Pt/C 0-D nanomaterials, even after 50 cycles. The promotional effect of Pt-Au nanorods may be attributed to the Au alloying effect and the 1-D morphology [3], favorably enhancing the ORR activity. On the other hand, based on the long-term measurement, it can be seen that both nanorods show the superior stability in 0.5 M H_2SO_4 solution.

Besides ORR performance, the CO-stripping results are examined in 0.5 M H_2SO_4 solution and compared in Figure 5. The Pt shell nanorods exhibit the best onset potential compared with the others, suggesting the surface Pt is favorable for oxidation of CO molecular and thus enhances the kinetics of CO stripping. However, for PtAu shell nanorods, the surface enrichment of Au may induce a deterioration of the CO oxidation than Pt/C. This can be explained by the DFT theory that a strong adsorption of CO on surface Pt sites owing to the presence of surface Au may cause the deterioration of the electroactivity [18].

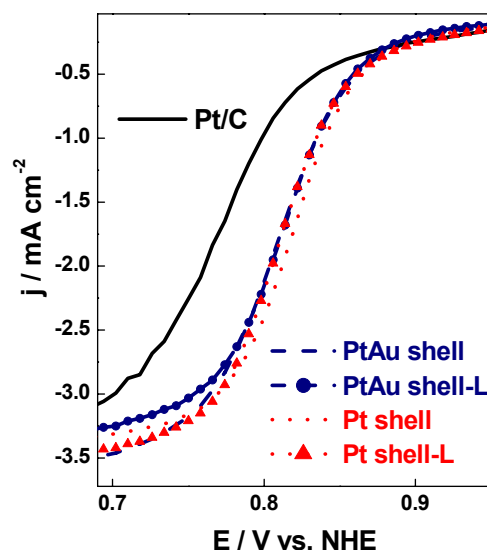


Figure 4: The LSV recorded in O_2 saturated 0.5 M H_2SO_4 for Pt-Au nanorods and Pt/C catalyst.

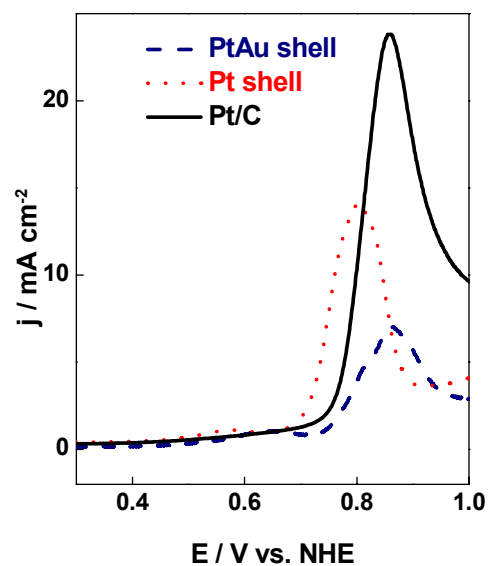


Figure 5: The CO stripping of Pt-Au nanorods and Pt/C catalyst in 0.5 M H_2SO_4 .

On the contrary, in terms of FAO activity shown in Figure 6, the PtAu shell nanorods, with surface Au enrichment, have superior FAO performance compared to Pt shell nanorods and commercial Pt/C. It can be seen that the existence of Au species on their surface can significantly enhance the FAO electrocatalytic activity, consisting with the results that PtAu/C nanoparticles with surface enrichment of Au have a positive effect on FAO compared to Pt/C and PtRu/C catalyst. Besides, a lower onset potential and large current density can be obtained for PtAu/C as the proportion of Au increases [19].

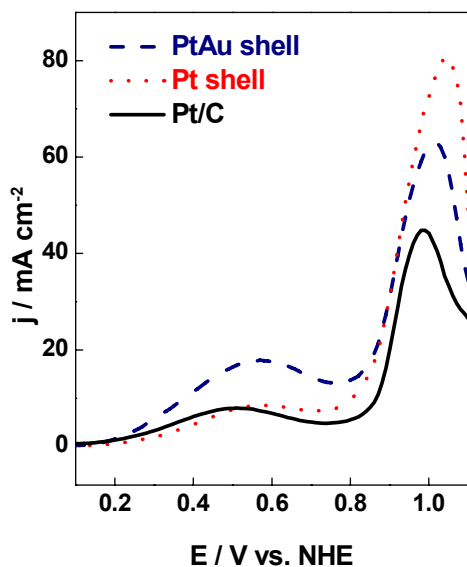


Figure 6: The forward scans of Pt-Au nanorods and Pt/C catalyst in the CVs for FAO in 2.0 M HCOOH and 0.5 M H₂SO₄.

4 CONCLUSIONS

In this study, carbon-supported Pt-Au nanorods with core/shell structures and excellent electrochemical performance are prepared successfully by a facile wet chemical reduction method. Due to the Au alloying and 1-D morphology, the ORR activity and long-term durability of Pt-Au nanorods are both better than those of commercial Pt/C nanoparticles. Besides, it can be observed that for Pt shell nanorods, the surface is completely composed of Pt species, exhibiting high CO oxidation activity. On the other hand, the surface of PtAu shell nanorods consists of Pt and Au species, which specifically benefit FAO. The promotional effect of Pt-Au nanorods may be attributed to the 1-D morphology, favorably enhancing the electrochemical activity of ORR, FAO and CO oxidation.

REFERENCES

- [1] B. Lim, M. Jiang, P. H. C. Camargo, E. C. Cho, J. Tao, X. Lu, Y. Zhu and Y. Xia, *Science* 324, 1302, 2009.
- [2] M. T. M. Koper, *Fuel cell catalysts*, Wiley Interscience, Hoboken, NJ, 2009.
- [3] C. Koenigsman, W. P. Zhou, R. R. Adzic, E. Sutter and S. S. Wong, *Nano Lett.* 10, 2806, 2010.
- [4] L. Cademartiri and G. A. Ozin, *Adv. Mater.* 21, 1013, 2009.
- [5] Y. Y. Shao, G. P. Yin and Y. Z. Gao, *J. Power Sources* 171, 558, 2007.
- [6] H. J. Kim, Y. S. Kim, M. H. Seo, S. M. Choi, J. Cho, G. W. Huber and W. B. Kim, *Electrochem. Commun.* 12, 32, 2010.
- [7] X. Yu and S. Ye, *J. Power Sources* 172, 145, 2007.
- [8] J. L. Gomez de la Fuente, J. San-Fabian, J. Sanza, M. A. Pena, F. J. Garcia-Garcia, P. Terreros and J. L. G. Fierro, *J. Phys. Chem. C* 111, 2913, 2007.
- [9] C. W. Liu, Y. C. Wei and K. W. Wang, *J. Colloid Inter. Sci.* 336, 654, 2009.
- [10] S. H. Sun, F. Jaouen and J. P. Dodelet, *Adv. Mater.* 20, 3900, 2008.
- [11] J. H. Choi, K. W. Park, I. S. Park, K. Kim, J. S. Lee and Y. E. Sung, *J. Electrochem. Soc.* 153, A1812, 2006.
- [12] N. Kristian and X. Wang, *Electrochem. Commun.* 10, 12, 2008.
- [13] W. Wang, Q. Huang, J. Liu, Z. Zou, M. Zhao, W. Vogel and H. Yang, *J. Catal.* 266, 156, 2009.
- [14] J. Luo, L. Y. Wang, D. Mott, P. Njoki, Y. Lin, T. He, Z. Xu, B. Wanjana, S. I-Im Lim and C. J. Zhong, *Adv. Mater.* 20, 4342, 2008.
- [15] A. Hamelin, *J. Electroanal. Chem.* 407, 1, 1996.
- [16] Y. Ma, H. Zhang, H. Zhong, T. Xu, H. Jin and X. Geng, *Catal. Commun.* 11, 434, 2010.
- [17] J. Jiang and B. Yi, *J. Electroanal. Chem.* 577, 107, 2005.
- [18] C. Song, Q. Ge and L. Wang, *J. Phys. Chem. B* 109, 22341, 2005.
- [19] N. Kristian, Y. Yan and X. Wang, *Chem. Commun.* 353, 353, 2008.